Forcing mechanisms of the Bay of Bengal circulation

P. N. Vinayachandran, Satish R. Shetye*, Debasis Sengupta and Sulochana Gadgil

Centre for Atmospheric Sciences, Indian Institute of Science, Bangalore 560 012, India
*National Institute of Oceanography, Goa 403 004, India

A state-of-the-art ocean general circulation model, set up for the North Indian Ocean and driven by climatological wind stress simulates most of the observed features of the near-surface circulation of the Bay of Bengal. The prominent features of the annual cycle are an anticyclonic gyre with a poleward East India Coastal Current (EICC) during February–May, and an equatorward EICC during October–December. During the summer monsoon, the coastal current flows poleward in the south and equatorward in the north. To identify the principal mechanisms governing this cycle, we carried out experiments with modified winds. When spatially uniform wind stress was applied only over the Bay, the circulation is similar to, but weaker than the observed, and can be linked to two coastal Kelvin wave pulses which originate along the eastern boundary of the Bay during the summer and winter monsoons. When the Bay is forced with observed winds, the wind stress curl strengthens the poleward EICC during February–May and the equatorward EICC during October–December. The principal contribution of equatorial winds is to generate the equatorward coastal current during the summer monsoon off the east coast of India.

1. Introduction

THE Indian Ocean has a unique geographic setting; it is bounded in the north by the Eurasian Land mass. This termination of the ocean in the tropics gives rise to spectacular seasonality in the overlying atmosphere and, consequently, in the ocean itself. North of 10°S the surface winds blow from the southwest during May–September and from the northeast during November–February. The ocean is primarily driven by winds, and under the influence of the seasonally reversing monsoon winds, the circulation in the Indian Ocean reverses twice during the year.

The response of the Indian Ocean to monsoon forcing has evoked considerable interest in the past. However, most of the attention has been focused on the western part of the Indian Ocean, which has a prominent seasonally reversing current viz. the Somali Current[1,2]. The rest of the basin has remained rather poorly observed and little studied. This is particularly true for the Bay of Bengal, which forms the northeastern part of the Indian Ocean. The Bay is not only of great oceanographic interest but it also plays an important role in maintaining and modulating the monsoon over the Indian region.

The Bay is markedly different from the Arabian Sea in two respects. Firstly, over the Arabian Sea, evaporation exceeds precipitation and it receives highly saline water from the Red Sea and from the Persian Gulf, making the salinity of the upper layer rather high. In contrast, over the Bay rainfall exceeds evaporation and the Bay also receives a large quantity of freshwater as river discharge, leading to an upper layer of less saline water for a large part of the year[3]. The surface waters in the Bay have such low salinity that the stratification in the upper layer is dominated by salinity gradients rather than temperature gradients[4].

Secondly, over a large part of the year the sea surface temperature (SST) of the Bay is above 28°C (ref. 5), which is the threshold SST for active generation of large-scale convection/precipitation[6]. On the other hand, the SST in the Arabian Sea, west of about 70°E, is below the threshold over most of the year. The SST is determined by the heat flux at the sea surface (which in turn depends on surface winds and on SST itself) and horizontal and vertical advection in the ocean. How SSTs higher than 28°C are maintained in the Bay is not yet clearly understood. Most of the low pressure systems, depressions and cyclones which give rainfall over the Indian region are generated over the Bay. The coupling of the monsoon atmosphere with the Bay must therefore play an important role in determining rainfall over the Indian region and its variability. Thus understanding the Bay is a challenging problem in the areas of ocean dynamics and coupled ocean–atmosphere systems.

During the last few years, new observations have been made in the Bay, by Shetye *et al.*[4,7,8] in the western Bay and by Murthy *et al.*[9] and Suryanarayana *et al.*[10] in the central Bay. These and earlier analysis of ship-drifts[11] show a distinct seasonal cycle of surface circulation[3]. A prominent feature of this seasonal cycle is the seasonally reversing coastal currents. The coastal current along the east coast of India flows poleward before the summer monsoon and equatorward during the winter monsoon season. During the summer monsoon there is a poleward current along the Indian coast in the southern part and an equatorward current in the northern part.

One of the major aims of ocean modelling studies is to simulate the observed seasonal variation in the circulation and understand it in terms of the response to the winds over the Bay as well as other regions. Both these aspects have been addressed so far using the relatively simple reduced gravity models, which assume that the ocean is made up of very few layers of which the lowest one is static. The studies of Potemra *et al.*[12] and McCreary *et al.*[13] (henceforth MKM) have shown that major features of the surface circulation are simulated by such models. Two types of waves have been shown to play a pivotal role in the time-dependent response of the Bay to the wind-forcing. These are the Rossby waves which occur everywhere in the oceans, and the Kelvin waves, which propagate along the coast. Equatorial Kelvin waves generated by winds over the equatorial Indian Ocean propagate eastward. On encountering the eastern boundary of the ocean, a part of the energy of these waves is transferred to coastal Kelvin waves. The latter move rapidly along the coastline of the Bay of Bengal and influence the circulation in the Bay.

On the question of forcing the circulation in the Bay, different mechanisms have been proposed involving winds over the Bay, and winds over the equatorial Indian Ocean, and Rossby and Kelvin waves. Potemra *et al.*[12] highlighted the role of planetary waves in setting up the seasonal circulation. Yu *et al.*[14] argued that these waves have their origin as equatorial Kelvin waves, implying that equatorial forcing alone can set up the observed annual cycle. MKM[13] highlighted the importance of coastal Kelvin waves and Rossby waves generated entirely in the Bay by local alongshore winds. Shetye *et al.*[7] have emphasized the role of winds over the open Bay. Recently, Shankar *et al.*[15] and McCreary *et al.*[16] have examined the roles of different mechanisms in an analytic model and in numerical experiments.

In this paper we address the problem of understanding the relative roles of different mechanisms in driving the circulation of the Bay using a state-of-the-art ocean general circulation model (OGCM) developed by Bryan[17] and Cox[18]. While general circulation models of the atmosphere have been used in our country for several years, this is the first implementation of an OGCM. We report the results of several experiments carried out with the Bryan–Cox model with two objectives. The first is to see how well the known features of the near-surface circulation in the Bay are reproduced when climatological monthly mean winds force the model. Second, we carry out numerical experiments aimed at constructing a simple, yet dynamically correct, picture of circulation in the Bay. These experiments also permit us to estimate the contribution of different mechanisms in driving the circulation in the Bay. The model set-up is briefly described in section 2. Section 3 discusses the annual cycle, comparing the model results with ship-drifts. Sensitivity of the model to horizontal resolution is examined in section 4. In section 5 the results of model runs with modified wind fields are examined. Section 6 summarizes the main findings.

2. The model set-up

The Bryan-Cox model, now commonly known as the Modular Ocean Model[19], solves the primitive equations on a finite difference grid using the method of Bryan[17] The model domain for the present study lies between 20°S–25°N and 40°E–100°E, with a no-slip condition on all boundaries. The horizontal grid spacing is 1° in both zonal and meridional directions. There are 15 levels in the vertical, of which 8 are in the top 100 m (Table 1). We have also made a run with a grid spacing of 1/3° to test the sensitivity to horizontal resolution.

Horizontal diffusivity and viscosity are set to 5×10^7 cm^2 s^{-1}. The scheme of Pacanowski and Philander[20] is used for vertical mixing. The model has realistic coastline geometry and topography as resolved by the Scripps topography[21]. The model is started from a state of rest with initial conditions for temperature and salinity obtained from the Levitus[22] climatology for January. At the surface the model is forced by the climatological wind stress of Hellerman and Rosenstein[23] (henceforth H&R). The surface boundary condition for temperature and salinity is of the relaxation type[24], with a relaxation time of 10 days. At the southern boundary, temperature and salinity are relaxed to their climatological values. It is integrated for four years and model fields during the fourth year are used for the discussion below.

Table 1. Vertical levels in the model

Level	Thickness (m)	Depth to the grid point (m)
1	10.0	5.0
2	10.0	15.0
3	10.0	25.0
4	10.0	35.0
5	10.2	45.1
6	10.9	55.7
7	13.5	67.9
8	21.4	85.3
9	42.5	117.3
10	90.7	183.9
11	184.1	321.3
12	336.6	581.3
13	542.7	1021.3
14	765.5	1675.4
15	941.8	2529.1

The geometry of the model is unrealistic with a closed southern boundary, no Indonesian throughflow, closed Malaca strait, lack of island chains and smooth bottom topography. There is no evidence that effects arising from 20°S influence near-surface circulation in the Bay. Similarly, the closing of the Indonesian passage is unlikely to affect the Bay of Bengal circulation because the Indo-Pacific throughflow is found to affect the circulation only to the south of the equator[13]. However, consequences of closing the Malacca Strait and lack of island chains in the model are not known. A deficiency of the model is the lack of river discharge, though it is partly accounted for by the surface boundary condition on salinity. Since the present study is the first attempt to study the Bay using an OGCM we decided to defer exploring the role of river discharge to the future.

3. The annual cycle

During May to September the southeast trades in the south Indian Ocean cross the equator near the African coast and turn southwesterly. In the Bay of Bengal and Arabian Sea the southwesterlies strengthen during June, reach their peak during July–August, start decaying during September, and vanish by October (Figure 1). During November–February northeasterly winds prevail north of the equator, turning northwesterly in the south. These winds reach their peak during December. In the Bay these winds die by the end of February (Figure 1), whereas in the Arabian Sea they persist till March. In general, the winds during November–February are much weaker than the summer monsoon winds.

Winds in the equatorial (5°S–5°N) Indian Ocean (EIO), east of 55°E, are relatively calm throughout the year except during the transition between the monsoons, April–May and October–November, when strong westerlies occur[25]. Due to these episodes, the annual cycle of the winds in the EIO has a significant semi-annual component. In contrast, the periodicity of winds in the Bay of Bengal is predominantly annual.

In response to the winds, circulation in the Bay exhibits a seasonal cycle both in surface currents and in deeper flow. The ship-drift climatology[11] provides a comprehensive view of the seasonal cycle of the surface currents in the Bay of Bengal. We first examine how well the model performs in simulating the upper layer circulation by comparing with ship-drifts.

Comparison with ship-drifts

During February–April ship-drifts in the Bay show (Figure 2 *a*, *b*) the presence of an anticyclonic (clockwise) gyre with a poleward East India Coastal Current (EICC). To the south of the gyre, approximately along 6°N, a westward current called the North Equatorial Current[26] (NEC) is present. Piecing together hydrographic data and climatologies[11,22] Shetye *et al.*[7] inferred that the poleward EICC in the Bay of Bengal[27] during February–May is a part of a seasonal anticyclonic gyre enveloping the entire Bay. The anticyclonic gyre, the EICC and the NEC are reproduced well by the model. The initial formation of the anticyclonic gyre in the model takes place in the northern Bay during January. The EICC forms by February (Figure 2 *a*) and is fully developed by March. During February, the northern part of the EICC is fed by a northwestward flow in the central Bay and the westward North Equatorial Current feeds into the southern part. The model EICC and the anticyclonic gyre are present up to level 10 (about 200 m). Typical speeds are in the range 15–30 cm s^{-1}. During February and March there is a northwestward flow in the southwestern Bay and during April a slow southward drift exists in the rest of the open Bay

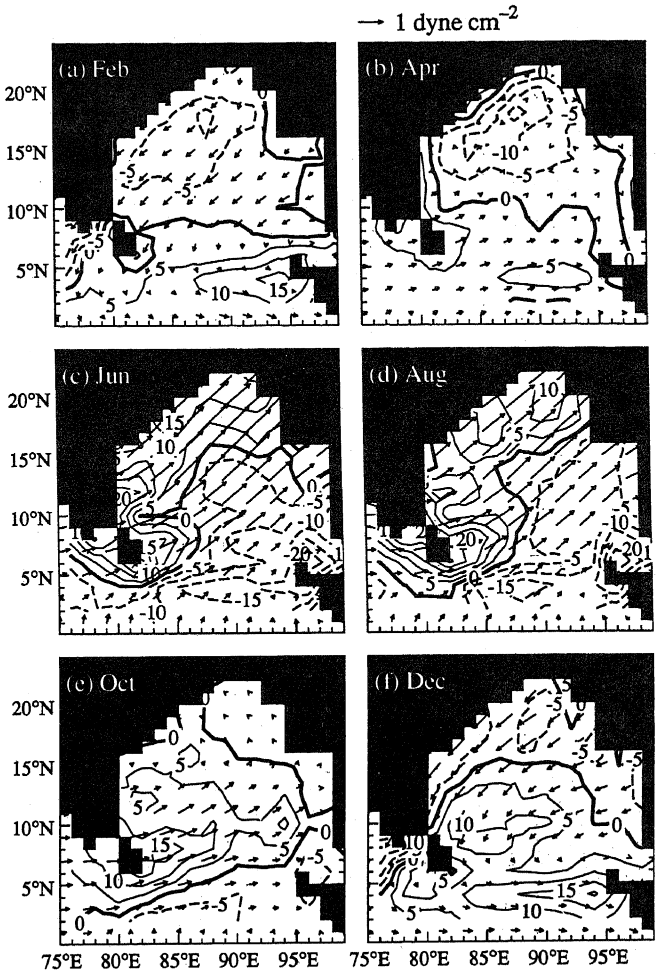

Figure 1. Bi-monthly maps of winds over the Bay of Bengal (H & R). Vectors represent wind stress. Contours represent wind stress curl; thick, dashed and continuous contours represent zero, negative and positive curl respectively. Contour interval is 5 dynes cm^{-3}.

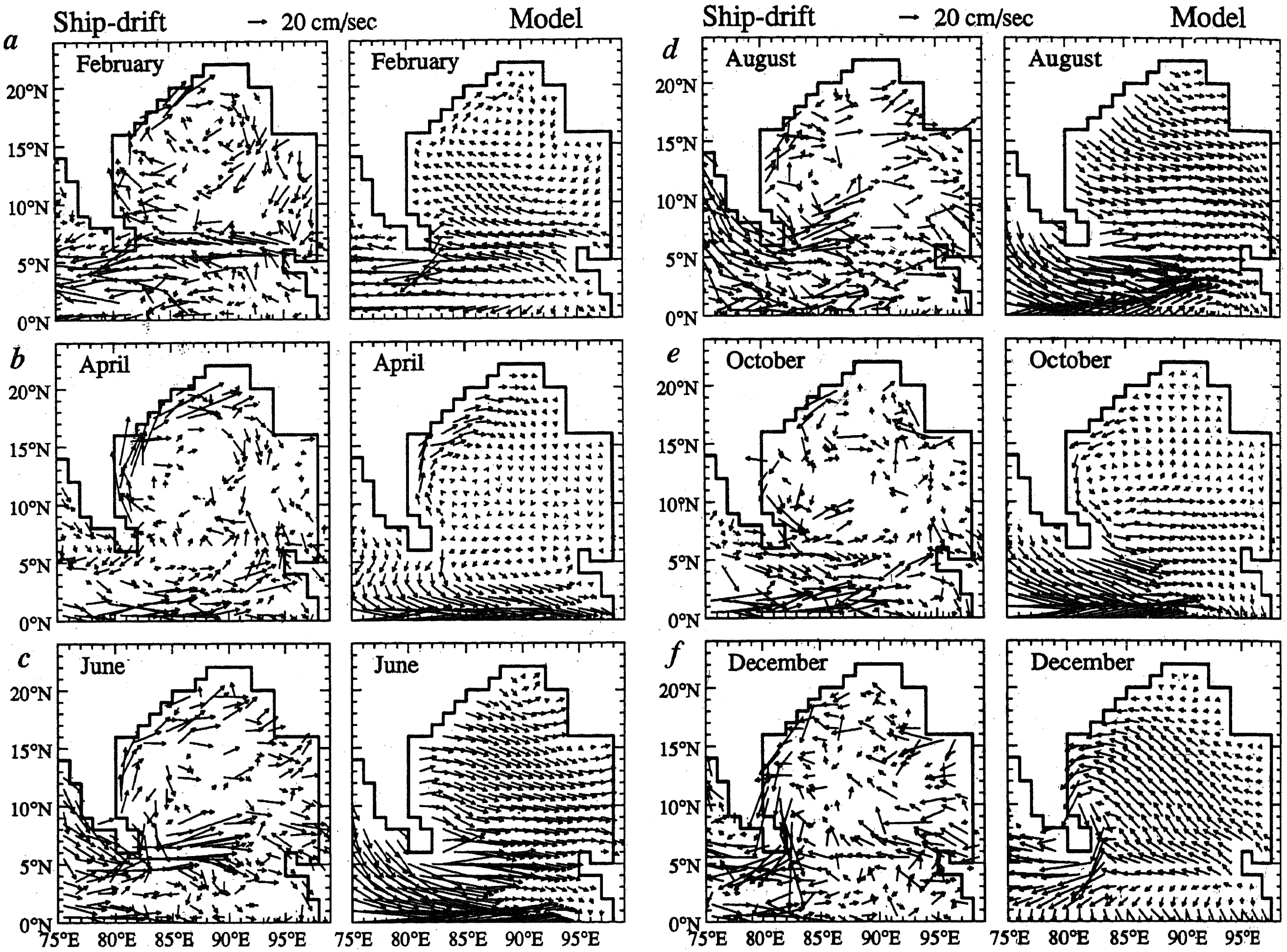

Figure 2. Comparison of the model currents at level 1 (5 m) with ship-drifts. Left panel shows ship-drifts and right panel shows model currents. Five day outputs from the model are averaged to construct monthly mean model currents. To project dominant currents a ship-drift vector was plotted only when the magnitude exceeded 5 cm s^{-1} and when there were more than 5 observations in a 1° box.

(Figure 2 *b*). The simulated open ocean flow is weaker than the ship-drifts. The ship-drifts suggest a northeastward flow in the southeastern Bay. This flow is very weak in the model. Further, the ship-drifts between 0 and 3°N are eastward, whereas the model flow is towards the southeast.

The ship drifts show that by May the anticyclonic gyre begins to break up and is no longer seen by June (Figure 2 *c*). A poleward coastal current is seen along the east coast of India during May–June but it cannot be associated with a gyre like in March–April. In the open Bay, in the north, large eastward ship drifts are observed during June–August (Figure 2 *c*, *d*). These are probably due to Ekman drift, i.e. directly wind-driven shallow currents, flowing at an angle to the right of the wind in the northern hemisphere. In the model also, an eastward flow is seen in the open Bay during this period. However, the model currents at the first three model levels (5, 15 and 25 m) appear to be dominated by Ekman flow[28], and hence do not compare well with observations. The model Ekman flow is too strong and makes too large an angle with the wind direction. The model eastward current south of Sri Lanka has shifted southward of the observed location. The prominent northeastward flow into the Bay at the termination of this eastward current is not simulated at all. The current along the east coast of India is also not simulated. Clearly the model needs to be improved for a more realistic simulation of the upper layer currents in this season.

Immediately below the layer dominated by Ekman flow (at 35 m), however, the currents along the east coast of India during May and June are well simulated by the model (Figure 3 *a*, *b*). At this level there is also a poleward current along the eastern boundary of the Bay. As summer progresses, this current propagates along the boundary of the basin with the coast to its right; by July it is an equatorward flow off the Orissa

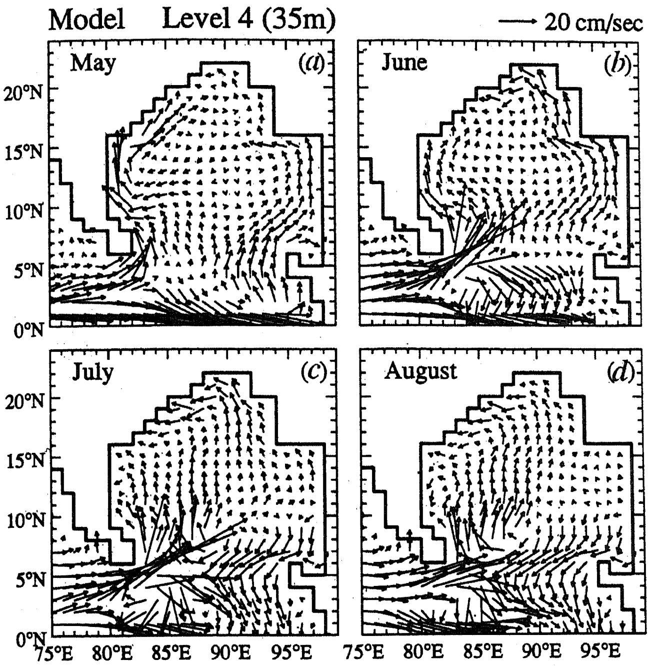

Figure 3. Model currents at level 4 (35 m) during (*a*) May, (*b*) June, (*c*) July, and (*d*) August.

coast. On the other hand, the poleward current along the east coast of India retreats and disappears by July. The flow field inferred from hydrographic observations along the western boundary of the Bay[4] supports the model simulation. There are no observations in the eastern part of the Bay to confirm the presence of the poleward current predicted by the model. The model northward flow in the open Bay in July at this level is consistent with observations[9].

Both model currents and ship-drifts suggest a cyclonic gyre during October–November. This gyre breaks up and a northwestward flow develops in the open Bay during November. Hydrographic data[8] during December also suggests a similar feature. The formation of a southward coastal current off the east coast of India takes place in the model during October (Figure 2 *e*), after the withdrawal of southwesterly winds. This southward coastal current is present till January.

In summary, we note that the overall pattern of surface currents in the model is consistent with ship-drifts. However, there are differences near the western and southern parts of the Bay during May–September, when the winds are strongest. Both the model level-1 currents and the observed surface circulation are best organized during March–April, when an anticyclonic gyre with a poleward EICC is present. There is also a period of organized cyclonic flow with an equatorward EICC, during October–November.

4. Sensitivity to horizontal resolution

Since the fundamental length scale of ocean motions, the Rossby radius of deformation, can be smaller than 1° in the latitude range of the Bay of Bengal, a better horizontal resolution is desirable. But the computational load rises steeply with increase in number of grid points and decrease in time step demanded by the numerical stability requirements. As a compromise we set up the model with a minimum spacing of 1/3° in the Bay of Bengal and in the EIO. With a grid spacing of 1/3°, most energetic small-scale features of the flow, including the equatorially trapped waves (which are crucial to the forcing mechanisms described in next section) can be expected to be well represented[29]. Horitontal eddy coefficients in this case are 2×10^7 cm^2 s^{-1}. To save computer time, the depth averaged flow – 'the barotropic component' – is suppressed. Since our interest in this study is limited to the upper layers, where the contribution from the depth averaged velocity is small, this is a reasonable strategy to adopt.

One immediate consequence of increasing spatial resolution to 1/3° is that the flow field acquires rich spatial structure with embedded eddy type flow pattern, particularly during February–March and June–September (Figure 4). The northwestward flow in the central Bay splits into two branches (Figure 4 *a*, *b*). The main branch turns northward to feed the EICC between 14°N and 17°N. A small branch forms a cyclonic eddy offshore of the EICC between 10°N and 13°N. During July two anticlockwise cells are present along the western boundary (Figure 4 *b*); the first is located off the Sri Lankan coast and the second off the southeast coast of India. How realistic is this fine structure? We really do not know, but there are references in the literature to similar, relatively small scale features in the Bay of Bengal circulation. Legeckis[27] observed in satellite derived SST that eddies characteristic of western boundary currents are present in the Bay of Bengal as well. Babu *et al.*[30] documented a subsurface cyclonic eddy along the western boundary during summer monsoon. The flow field along the western boundary during the summer monsoon consists of several cells in the observations of Shetye *et al.*[4]. It is hoped that the present fine-resolution model results would serve as a guideline to plan future field experiments in this direction. Since the wind stress used to force the model does not have the small spatial scales seen in Figure 4 *a*, *c*, it is suggested that these small-scale structures in the flow field are born from ocean dynamics. This needs to be confirmed through further study.

5. Forcing mechanisms

Modelling studies during the last few years[12–16] have shown that the main features of the annual cycle of cir-

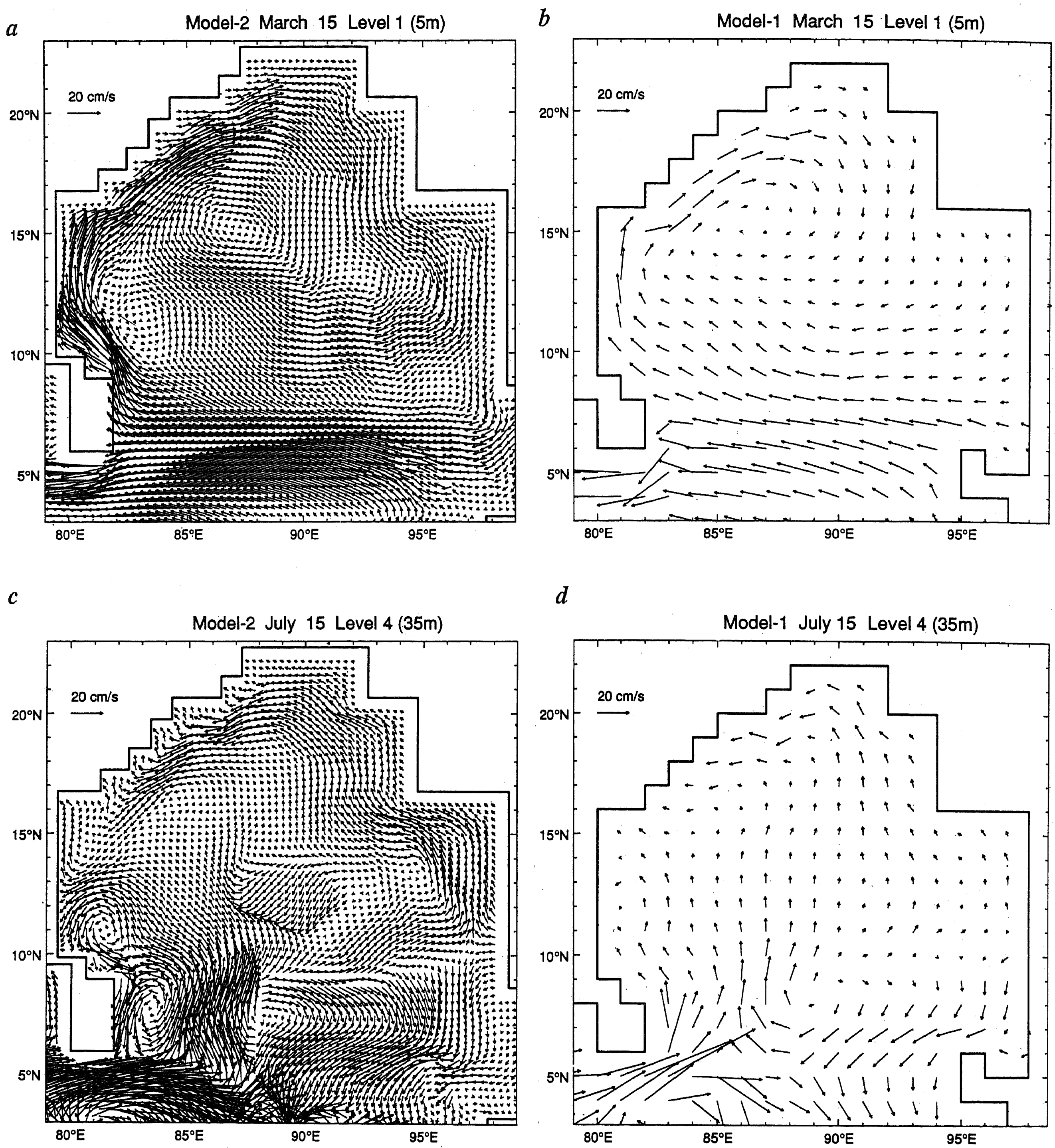

Figure 4. *a*, Currents during March at the first model level (5 m) from the model with a horizontal grid of 1/3° in the Bay of Bengal and in the EIO; *b*, Currents during March at the first model level (5 m) from the model with a horizontal grid spacing of 1° over the entire model domain; *c*, Currents during July at the fourth model level (35 m) from the model with a horizontal grid spacing of 1/3° in the Bay of Bengal and in the EIO; *d*, Currents during July at the fourth model level (35 m) from the model with a horizontal grid spacing of 1° over the entire model domain.

culation in the upper Bay can be understood in terms of coastal Kelvin waves along the periphery of the Bay and westward-propagating Rossby waves. The mechanisms that have been identified as generating the Kelvin waves are alongshore winds in the Bay[13] and equatorial processes[12,14]. Rossby waves are generated in the Bay either by Kelvin waves moving along the eastern boundary of the Bay or by the vorticity of the winds (wind stress curl) over the Bay. We thus have three mechanisms – longshore winds, wind stress curl and equatorial processes – that determine the annual cycle of circulation in the Bay.

In this section we report results of numerical experiments conducted to assess the relative roles of these forcing mechanisms. The model described in section 4 was used for these experiments. In the first experiment winds everywhere except the Bay were switched off; the winds over the Bay being averaged in space to eliminate wind stress curl. The purpose of this experiment was to examine what aspects of the circulation in the Bay can be reproduced with spatially uniform, but seasonally varying winds. In the second experiment, winds were again switched off everywhere except the Bay; the wind stress over the Bay, however, was taken from the monthly mean wind stress climatology[23]. In the third experiment winds everywhere were from climatology. The difference between the velocity field in the third and second experiments allows us to identify the contribution to the Bay from elsewhere in the Indian Ocean, primarily from the equatorial belt.

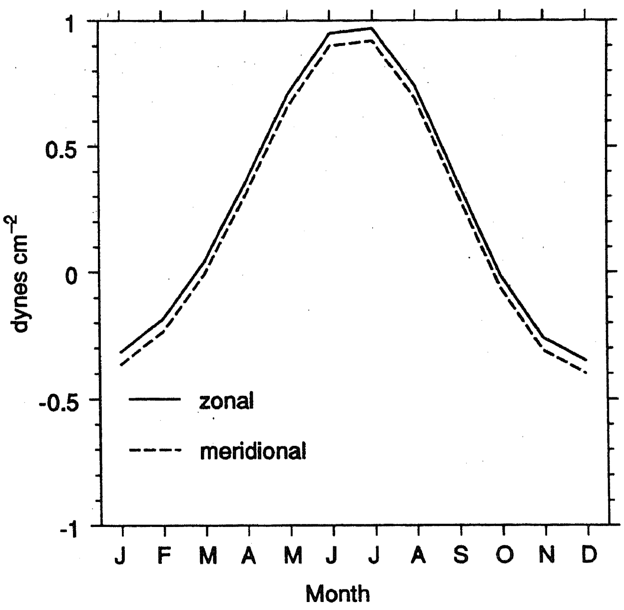

Figure 5. Annual cycle of zonal (full line) and meridional components (dashed line) of simplified spatially uniform wind stress.

Circulation in the Bay due to curl-free winds over the Bay

Convergence (divergence) in the upper ocean due to wind stress arising from a wind field that possesses curl, induces Ekman pumping (suction) in the deep ocean. Wind stress in the presence of the β-effect (variation of the coriolis parameter with latitude) also gives rise to Ekman pumping (suction)[31]. The major contribution to the Ekman pumping (suction) comes from the curl of the wind stress, the latter mechanism being significant mainly near the equator. We have constructed a simplified wind field over the Bay (Figure 5) by averaging in space the amplitudes of the annual and semi-annual harmonics of the climatological[23] wind stress. The annual and semi-annual harmonics were calculated using a least-square fit to monthly-mean wind stress[23].

The wind stress shown in Figure 5 was applied only over the region north of 9°N. South of this latitude the stress was decreased linearly to zero at 5°N. This tapering of wind stress introduces curl in the region 5–9°N. In the discussion below, we examine only the region north of 10°N. Shown in Figure 6 are velocities at 35 m, i.e. at a depth where Ekman velocity does not dominate the flow field.

The wind-field shown in Figure 5 essentially consists of two regimes. The first, made of southwesterly winds is stronger and starts building up during April. In response, a Kelvin wave pulse is generated along the eastern boundary (Figure 6 *b*). As the winds strengthen, the velocity field associated with the Kelvin wave strengthens. Kelvin waves can radiate Rossby waves offshore. By June (Figure 6 *c*), the Rossby wave radiated by the Kelvin wave can be seen as far west as 90°E. In addition, a patch of westward velocity can be seen west of about 87° E between 12 and 15° N. For the wind field used here, the only mechanism that can give rise to such a patch is Ekman suction due to β-effect. The upwelling favourable winds along the western boundary drive a poleward EICC there. This current weakens during July, although the wind stress peaks then. This is caused by the arrival of the downwelling Kelvin wave from the eastern boundary (Figure 6 *c*). The downwelling Kelvin wave is modified by the local upwelling favourable winds. In the northern part of the coast the downwelling wave dominates; as one moves southward, however, local forcing overwhelms it.

The southwesterly winds weaken during August. Seeking equilibrium with weakening winds, the velocity associated with the Kelvin wave at the eastern boundary falls to zero, and the flow then turns southward (Figure 6 *d, e*). This starts an upwelling phase of the Kelvin wave along the eastern boundary of the Bay. The southwesterlies withdraw during September and October, and the Kelvin wave along the eastern boundary has southward velocity along the entire coast (Figure 6 *e*).

During August the northward velocity associated with the Rossby wave radiated by the downwelling Kelvin wave (April–July) covers the entire Bay (Figure 6 *d*). As the velocity associated with the Kelvin wave at the eastern boundary turns southward, the velocity associated with the westward moving Rossby wave also turns southward (Figure 6 *e*). A region of weak flow separates

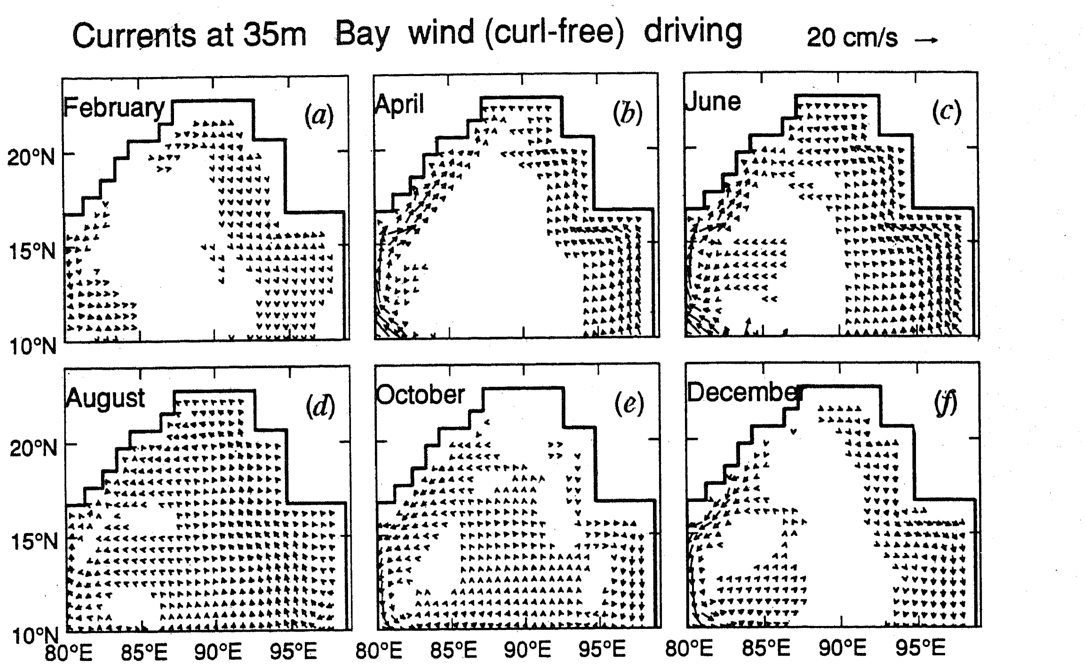

Figure 6. Currents at 35 m for the run with wind stress shown in Figure 5. The wind stress was applied only over the Bay of Bengal. A current vector was plotted only when the magnitude exceeded 2 cm s^{-1}.

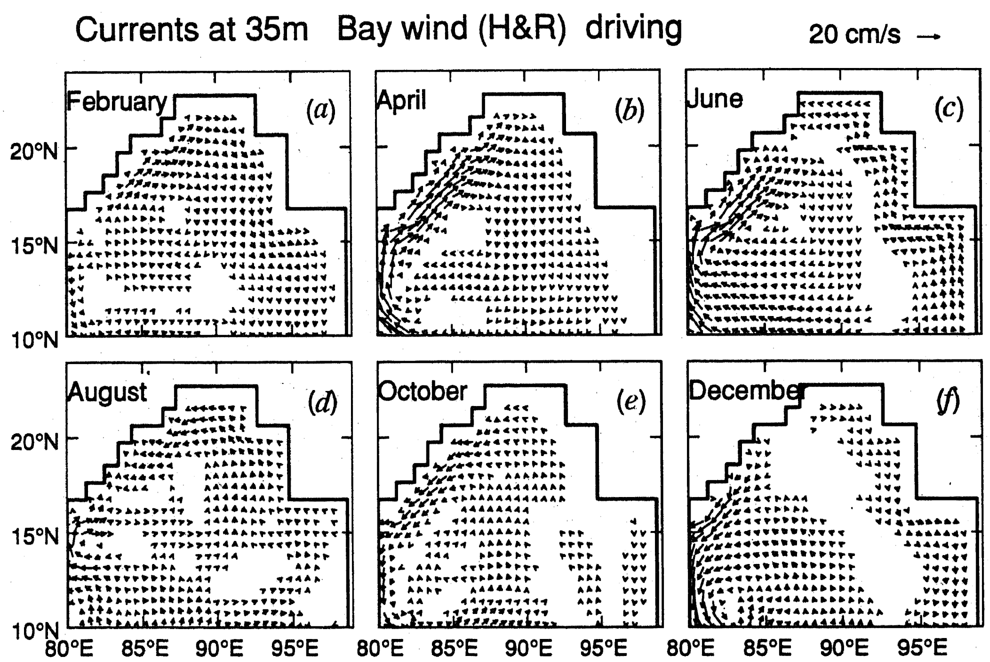

Figure 7. Same as Figure 6 but for the run with H & R winds applied only over the Bay.

(Figure 6 *e*) the regions of northward and southward velocities; the latter is seen only close to the coast.

The decrease of southwesterly winds also affects the flow along the western boundary: the locally driven poleward current weakens (Figure 6 *d*). As the southwesterly winds collapse, adjustment to the new wind field leads to the southward current (Figure 6 *e*), a process highlighted by MKM. Another mechanism that adds to the southward current is the reflection of the leading edge of the Rossby wave. Upon reflection this wave produces a narrow band of southward velocity. This reflected Rossby wave has a smaller wavelength.

The northeasterly winds are most intense during November–December. In response, an upwelling Kelvin wave forms along the eastern boundary. It is weaker than the downwelling Kelvin wave during April–July (compare Figure 6*f* with Figure 6*c*) because the wind stress is weaker.

During November, the Rossby wave radiated by the downwelling Kelvin wave of the summer monsoon is still present in the central Bay. This is seen as the westward migration of a patch with northward velocity, its reflection from the western boundary and the resulting southward EICC. In the eastern half of the Bay the Rossby wave pulse radiated by the upwelling Kelvin wave is present (Figure 6*f*). However, there is no indication of this Rossby wave crossing the Bay to have an impact on the western boundary. This is because the Rossby wave packet is weak and gets dissipated by the time it reaches the central Bay. Along the western boundary the northeasterly winds contribute to an equatorward flow during November–January (Figure 6*f*). By March the winds collapse; adjustment to the new winds leads to the formation of the poleward EICC.

Comparing Figures 6 and 2 we see that the overall pattern of near surface circulation has been reproduced well in this run with simplified winds. The process that was most active in this run was the generation of Kelvin wave pulses along the eastern boundary of the Bay. An important difference between this run and the one discussed in section 3 is that the circulation is weak in the former, implying that other mechanisms must be present to enhance the circulation.

Circulation due to winds over the Bay

In this experiment the model was forced by the annual cycle of H & R wind stress only over the Bay of Bengal. The purpose of this experiment was to examine the circulation in the Bay in the absence of equatorial wind forcing. An important difference between the run in the previous sub-section and the present run is that now Ekman suction from curl of wind stress is present. The simulated currents at 35 m are shown in Figure 7. Below we discuss the changes seen in this figure from the circulation described in section 5.1

During March–April, the main difference from the previous run is that there is a well developed anticyclonic gyre with a poleward EICC (Figure 7*b*). Because of the gyre, the velocity field in the open Bay is stronger (compare Figure 6*b* with Figure 7*b*). The primary cause of the difference between these figures is the contribution from wind stress curl. The currents along the eastern Bay are prominent in the case of curl-free driving due to the alongshore winds.

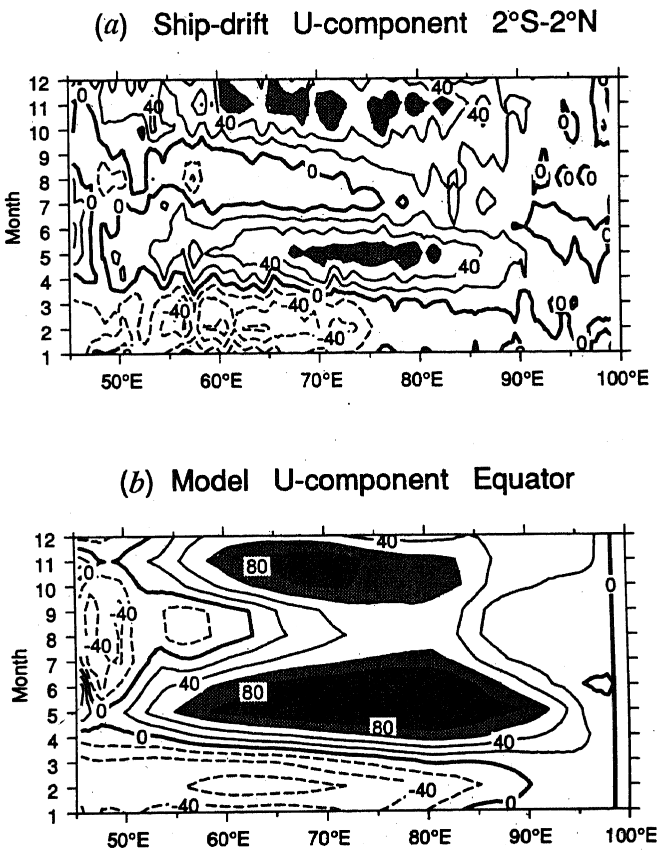

Figure 8. Time longitude sections of zonal velocity (i) in the equatorial region (averaged between 2°S and 2°N) from the ship-drifts and (ii) along the equator from the model. Thick line represents zero contour and dotted contours represent westward flow. Eastward velocity greater than 60 cm s^{-1} is shaded to show the equatorial jets.

During November–January, the southward EICC is stronger in the present run (compare Figure 6*f* with Figure 7*f*). The principal cause behind this change is a patch of wind stress curl which forms over the region off Sri Lanka during October. The northward flow in the open Bay seen in the earlier experiment was the result of the Rossby wave radiated from the eastern boundary. Now, in the presence of wind stress curl, the contribution to the velocity field from that Rossby wave is increased due to the contribution from wind stress curl. The net result is a strengthening of the equatorward EICC.

Thus, the presence of wind stress curl strengthens the EICC by generating two gyres: an anticyclonic gyre during March–May in the Bay and a cyclonic gyre off the coast of southern India during the winter.

Circulation due to winds over the equatorial Indian Ocean

The source of all equatorial effects in the Bay is the equatorial Kelvin wave. To ensure that equatorial effects are properly accounted for, it is necessary that equatorial circulation be correctly simulated by the model.

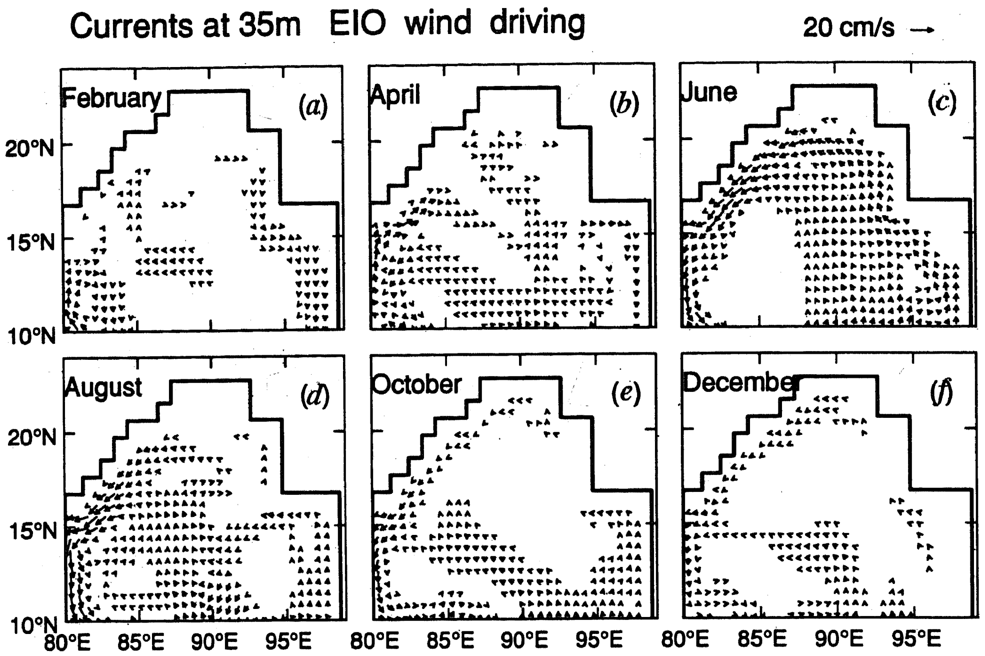

Figure 9. Currents at 35 m due to equatorial processes. This is calculated by subtracting the model result with winds (H & R) only over the Bay from the model result with winds (H & R) over the entire model domain. A current vector was plotted only when the magnitude exceeded 2 cm s^{-1}.

This can be seen in Figure 8 *a*, *b*, which shows the zonal component of monthly mean ship-drifts[11] and zonal velocity from the model. There is good resemblance between Figure 8 *a* and *b*, implying that equatorial circulation has been reasonably well reproduced. In particular, during April–May and October–November strong eastward jets similar to those first noted by Wyrtki[32] occur in the model. Note that MKM were unable to simulate the fall jet.

To study the impact of equatorial processes on the Bay of Bengal circulation, the velocity field in the run with winds only over the Bay was subtracted from that with winds over the entire model domain. The resulting velocity field is shown in Figure 9.

The velocity field in the Bay associated with equatorial forcing is weak (Figure 9). The most significant result of this driving is an equatorward current during the summer monsoon. This current is opposite in direction to those seen in the earlier two experiments (compare Figure 9 *c*, *d* with Figure 7 *c*, *d* and Figure 6 *c*, *d*).

In brief, the numerical experiments carried out here show that we can understand the annual cycle of circulation in the Bay in terms of the following: (i) Two Kelvin wave pulses generated by alongshore winds in the coastal region of the Bay, mainly its eastern boundary. (ii) Circulation set up by wind stress curl over the Bay; primarily an anticyclonic gyre during March–May and a cyclonic gyre in the southwestern Bay during October–December. (iii) A weak circulation set up by equatorial forcing, whose main effect is to reduce the strength of the poleward current during the summer monsoon.

6. Conclusions

The results of numerical experiments discussed above show the usefulness of the OGCM in simulating and understanding the upper-layer circulation in the Bay of Bengal. The model reproduces most of the features seen in the available data sets. The results of the numerical experiments allow us to construct the following hierarchy of processes dominating the circulation in the Bay:

i) *Coastal Kelvin wave pulses generated along the boundary region, primarily the eastern boundary*

The more important of the two pulses is the downwelling pulse generated with the onset of the southwesterly winds. Its impact on the coastal current is most important in the north during the summer monsoon. The second pulse, an upwelling event, occurs during the winter monsoon and it generates a poleward EICC during March. Both these pulses contribute towards circulation in the Bay by radiating Rossby waves. However, it is necessary to invoke other mechanisms to explain all the features of circulation.

ii) *Rossby waves generated by Ekman suction over the Bay*

The main function of this mechanism is to strengthen the EICC by generating an anticyclonic gyre during March–May and a cyclonic gyre during the winter monsoon.

iii) *Effects derived from the equatorial region*

The most significant effect of this forcing is an equatorward current off the east coast of India during the summer monsoon. This current is opposite to that driven by the winds over the Bay.

It is clear that more modelling studies are required, for instance, to improve the simulation of the currents during the summer monsoon. Above all, a well planned observational programme is a must for further progress in understanding the dynamics and thermodynamics of the Bay of Bengal and its coupling with the monsoon. Although theoretical studies suggest that low-frequency Rossby and Kelvin waves are crucial to the circulation, their presence has not been established in the field. The impact of freshwater driving and the nature of space-time variation of the stratification of the Bay also needs to be elucidated with the help of more observations. None of the model studies so far have taken into account the freshwater input into the Bay explicitly. In future modelling studies, the important problem of understanding the role of buoyancy driving in the circulation of the Bay will be addressed.

1. Schott, F., *Prog. Oceanogr.*, 1983, **12**, 357–382.
2. Luther, M. E. and O'Brien, J. J., *Prog. Oceanogr.*, 1985, **14**, 353–385.
3. Vinayachandran, P. N., Seasonal Cycle of the Hydrography and Circulation of the Bay of Bengal, M Sc (Engg.) Thesis, Indian Institute of Science, Bangalore, 1992, pp. 61.
4. Shetye, S. R., Shenoi, S. S. C., Gouveia, A. D., Michael, G. S., Sundar, D. and Nampoothiri, G., *Cont. Shelf. Res.*, 1991, **11**, 1397–1408.
5. Vinayachandran, P. N. and Shetye, S. R., *Proc. Indian Acad. Sci. (Earth Planet. Sci.)*, 1991, **100**, 165–175.
6. Gadgil, S., Joseph, P. V. and Joshi, N. V., *Nature*, 1984, **312**, 141–143.
7. Shetye, S. R., Gouveia, A. D., Shenoi, S. S. C., Sundar, D., Michael, G. S. and Nampoothiri, G., *J. Geophys. Res.*, 1993, **98**, 945–954.
8. Shetye, S. R., Gouveia, A. D., Shankar, D., Shenoi, S. S. C., Vinayachandran, P. N., Sundar, D., Michael, G. S. and Nampoothiri, G., *J. Geophys. Res.*, 1996, **101**.
9. Murthy, V. S. N., Sarma, Y. V. B., Rao, D. P. and Murthy, C. S., *J. Mar. Res.*, 1992, **50**, 207–228.
10. Suryanarayana, A., Murthy, V. S. N. and Rao, D. P., *Deep Sea Res.*, 1993, **40**, 205–217.
11. Cutler, A. N. and Swallow, J. C., *Surface Currents of the Indian Ocean (to 25°°S; 100°E): Compiled from Historial Data Archived by the Meteorological Office, Bracknell, U.K*, Rep. 187, 36 charts, 8 pp. 1984 Inst. of Oceanogr. Sci. Wormley, U.K.
12. Potemra, J. T., Luther, M. E. and O'Brien, J. J., *J. Geophys. Res.*, 1991, **96**, 12667–12683.
13. McCreary, J. P., Kundu, P. K. and Molinari, R. L., *Progr. Oceanogr.*, 1993, **31**, 181–244.
14. Yu, L., O'Brien, J. J. and Yang, J., *J. Geophys. Res.*, 1991, **96**, 20449–20454.
15. Shankar, D., McCreary, J. P., Han, W. and Shetye, S. R., *J. Geophys. Res.*, 1996, **101**, 13975–13991.
16. McCreary, J. P., Han, W., Shankar, D. and Shetye, S. R., *J. Geophys. Res.*, **101**, 13993–14010.
17. Bryan, K., *J. Comput. Phys.*, 1969, **4**, 347–376.
18. Cox, M. D., *A Primitive Equation 3-Dimensional Model of the Ocean*, GFDL Ocean Group Tech. Rep. No. 1 GFDL/NOAA, Princeton University, Princeton, New Jersey, 1984, pp. 141.
19. Pacanowski, R. C., Dixon, K. and Rosati, A., *The GFDL Modular Ocean Model Users Guide*, GFDL Ocean Group Tech. Rep. No. 2, 1991.
20. Pacanowski, R. C. and Philander, S. G. H., *J. Phys. Oceanogr.*, 1981, **11**, 1443–1451.
21. Gates, W. L. and Nelson, A. B., *A New (Revised) Tabulation of the Scripps Topography on a 1° Global Grid. Part I: Terrain Heights*. 1975, Tech. Rep. R-1276-1-ARPA, The Rand Corporation, 1975, pp. 132.
22. Levitus, S., *Climatological Atlas of the World Ocean*, NOAA Prof. Pap. 13, US Government Printing Office, Washington, DC, 1982, pp. 173.
23. Hellerman, S. and Rosenstein, M., *J. Phys. Oceanogr.*, 1983, **13**, 1093–1110.
24. Haney, R. L., *J. Phys. Oceanogr.*, 1971, **1**, 241–248.
25. Knox, R. A., *Deep-Sea Res.*, 1976, **23**, 211–221.
26. Molinari, R. L., Olson, D. B. and Reverdine, G., *J. Geophys. Res.*, 1990, **95**, 7217–7238.
27. Legeckis, R., *J. Geophys. Res.*, 1987, **92**, 12974–12978.
28. Carrington, D. J., *Meteorol. Mag.*, 1991, **120**, 213–223.
29. Philander, S. G. H., Hurlin, W. J. and Pacanowski, R. A., *J. Phys. Oceanogr.*, 1986, **13**, 18–37.
30. Babu, M. T., Kumar, S. P. and Rao, D. P., *J. Mar. Res.*, 1991, **40**, 403–410.
31. Pedlosky, J., *Geophysical Fluid Dynamics*, Springer–Verlag, New York, 1979, pp. 624.
32. Wyrtki, K., *Science*, 1973, **181**, 262–264.

ACKNOWLEDGEMENTS. We thank D. Shankar for several discussions. The computations were carried out at the Supercomputer Education and Research Centre of IISc. We thank Drs K. Dixon and R. Pacanowski for providing MOM and Dr P. S. Swathi for his help in obtaining MOM data files. The NIO contribution number of this paper is 2498.

Received 30 May 1996; revised accepted 28 September 1996